Indonesian Journal of Electrical Engineering and Computer Science
Vol. 27, No. 3, September 2022, pp. 1388~1396
ISSN: 2502-4752, DOI: 10.11591/ijeecs.v27.i3.pp1388-1396

Enhancement of motor speed identification using artificial neural networks

Arshad B. Salih[1], Zuhair Shakor Mahmood[1], Ardm Haseeb Mohammaed Ali[2], Ali Najdet Nasret[1]
[1]Electronic Department, Kirkuk Technical Institute, Northern Technical University, kirkuk, Iraq
[2]Computer Techniques Department, Imam Ja'afar Al-Sadiq University, Baghdad, Iraq

Article Info

Article history:

Received Mar 24, 2022
Revised Jun 11, 2022
Accepted Jul 4, 2022

Keywords:

Ant colony algorithm
Back propagation
Direct torque control
Neural network
Speed identification

ABSTRACT

In this study have been utilized a modified version of ant colony optimization to improve the thresholds of neural networks and weights by including the rank- weight approach. Furthermore, this technique easily overcome the drawbacks speed up convergence into the minimum while training the back propagation neural network. The improved ant colony optimization-back propagation neural. not only has the capacity to map extensively, but it also enhances operating efficiency noticeably, according to the simulation findings. The simulation results revealed that the speed sensor replaced with the ant colony optimization rw-optimized back propagation neural network - speed identification and motor's speed determined using this approach the result is satisfactory.

Corresponding Author:

Ali Najdet Nasret
Electronic Department, Kirkuk Technical Institute, Northern Technical University
Kirkuk, Iraq
Email: alinajdet@ntu.edu.iq

1. INTRODUCTION

Direct torque control is presently the most successful control methods in alternating current timing technology due to its simple control structure and lower reliance on rotor parameters, for example [1], [2]. Speed sensors are often employed in direct torque control (DTC) systems to monitor rotational speed in closed-loop control, but their usage diminishes system dependability and increases equipment costs; in addition, they can- not be utilized in some situations, such as damp and dusty, when they are not reliable at all [3], [4]. Hence, the DTC based on speed sensor less technology has been detected by the general public. For the localization of the back propagation neural network model's speed identification approach, it still has several weaknesses, such as sluggish con stringency speed, fast convergence to local minimum points and a poor capacity to generalize [5], [6]. Despite these drawbacks, the back propagation neural network model has been extensively employed in recent years [7], [8]. As a result, optimizing the back propagation neural network has long been a major focus of study.

The ant colony optimization is a novel stochastic global optimization technique based on the notion of colony intelligence. This method was generated via looking for the ant's eating habits and it is simple to execute [9], [10]. This work uses a modified ant colony optimization , the weight-rank based ant colony optimization, which out- performs the standard ant colony optimization in terms of both time and derivation efficiency. With ant colony optimization and the neural network, you have a network that is capable of mapping a large area and improving global convergence performance. In neural network weights and thresholds optimization, it demonstrates excellent qualities. It is a powerful tool [8], [10]. This integrated approach was able to properly determine the motor's rotational speed in a simulated experiment using DTC [11], [12]. As a result, we may replace the DTC system's speed sensor with ant colony optimization rw-back propagation neural network-based speed identification and perform direct toque control for speed sensor less operation [13], [14].

2. SPEED IDENTIFICATION MODEL OF DIRECT TOQUE CONTROL

In recent years,the theory of DTC of induction motor has grown rapidly because of its rapid reaction to flux linkage and torque [4], [15] as well as its minimal reliance on the rotor parameters. in the direct toque control system theory the equations below describe the relationship of the static two-phase coordinate system between voltage,current and speed:

$$\{u\alpha, i\alpha, i\beta, u\beta\} \dashrightarrow \omega \tag{1}$$

non-linear mapping created using newral network. There are four inputs and four outputs, as shown in (1), the inputs are i_β, i_α, u_β and u_α. This means that the speed sensor may be changed. Speed identifi- cation using NN may be used to generate a speed signal that can be used as a feedback speed signal [16]-[18]. Also developed a speed sensor less DTC solution.

3. AN ALTERED VERSION OF THE ANT COLONY OPTIMIZATION NN

3.1. Back propagation neural network

There are many ways to reduce the mean square error of a back propagation network, but one way to do so is to distribute errors backwards until the error confessional request is reached, is to reduce the threshold and weights values of neural networks using this method. The back propagation (BP) neural network has several advantages, such as its capacity to generalize and its ability to map non-linearly, but it also has some drawbacks, such as its sluggish con stringency speed and its tendency to fall into local optimization. It is possible to see how the BP neural network is structured in the Figure 1.

The back propagation neural network's mathematical model is:

$$\begin{aligned} y_j &= f\sum W_{ij}X_j - \vartheta_j = f(nte_j) \\ O_I &= f\sum_j^i W_{ij}X_j - \vartheta_j = f(nte_I) \end{aligned} \tag{2}$$

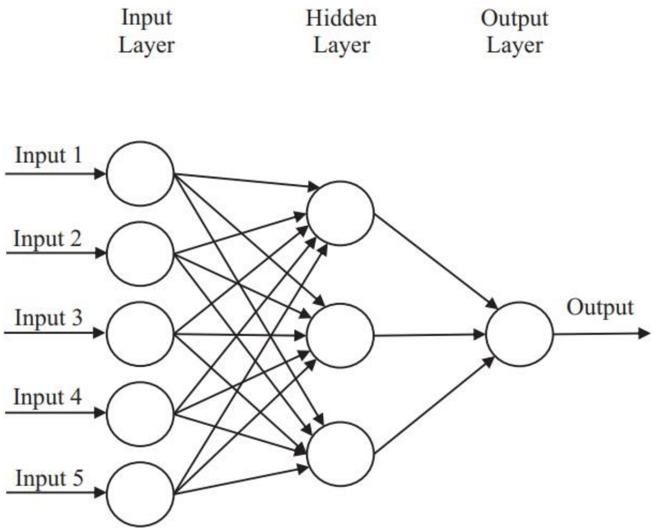

Figure 1. The BP neural network's structure

there are three floors nodes: the output node is xi Ol and input node is xi, then between this nodes there have a one hidden nodes is yj. In neural networks, the weights between hidden nodes and input nodes are wij the thresholds are θj. There is a threshold value wlj for the weights between output nodes and hidden nodes in neural networks is:

$$\vartheta_I net_j = w_{ij}x_i - \vartheta_j, net_I = W_{Ii}y_j - \vartheta_I$$

3.2. Ant colony optimization that been adjustment

3.2.1. The fundamental of ant colony optimization

The ant colony optimization algorithm, a particular number of ants are randomly placed in N cities and the pheromone of every route is meant to be equal at this moment [19], [20]. Ants pick their next city based on the pheromone concentration of each route as they go across the countryside. ants pick their transfer routes according to the transfer probability between adjacent ant colonies [21], [22]. As soon as one round of circulation is complete, ants release a little amount of pheromone throughout the paths. Once the ants had established a path of travel, the mystery of how they got there had been solved. The best solution is found once all of the ants have completed their circuits [23], [24].

As you can see, the essential ant colony optimization formulae are as:

$$P_r^k(t) = \frac{\tau_j^k(t)}{\sum_{g=1}^{N} \tau_g(t)} \tag{3}$$

$$\tau_j(t) = (1-\rho)\tau(t) + \rho\Delta\tau_j(t) \tag{4}$$

$$\Delta\tau_j(t) = \sum_{k=1}^{h} \Delta\tau_j^k(t) \tag{5}$$

$$\Delta\tau_j^k(t) = Q/L_N \tag{6}$$

at no. (pheromone) concentration LN is the distance between two places and t time at L_N is $\tau_j(t)$. P_r^K is the chance that ant No. k will transmit his pheromone at t time at L_N. Volatility coefficient ρ and constant Q are used to describe the rate at which a pheromone adjusts to a new environment.

3.2.2. Adaptive ant colony optimization that has been modified (ant colony optimization)

Increasing the volatility coefficient ρ will lower the global search capability of the approach in the context of multiple cities [25]. With a reduction in ρ, the method’s global searching power increases as a result. However, the rate of constricting will be slowed as a result of this.

Ant colony optimization may easily reach its apex if $L_N \geq Lmin$ is true. As a result, we may alter the value of the volatility coefficient, which is an adaptive ant colony optimization algorithm (ant colony optimization) [26], [27]. After the changes, To do a certain task (p):

$$0.95\rho(t), if\ 0.95\ \rho(t)\ >\ \rho_{\ min}\rho_{\ min} \tag{7}$$

if $L_N < Lmin$ As a rule, all parameters remain the same.

3.2.2. Ant colony optimization on the basis of weight-rank (ant colony optimization)

The underlying principle of ant colony optimization-rank-weight is to rank the routes obtained after each ant completes a single cycle in terms of length. It is the length of the routes taken in the process of circulation that determines how much each ant contributing to pheromone regeneration can do. The more the ant contributes, the shorter the journey is. According to ant circumference system model, a weight coefficient is to be regenerated based on the changes in the pheromone concentration and the ant No.k is the best No.k. So we’ve dubbed it the ant circumference system model. A worldwide approach to rebuild ant colonies is achieved by each individual ant participating. The same superior outcome may be achieved with fewer iterations. Solving large-scale problems becomes much easier with this approach, which may save a significant amount of computational effort. Using the revised:

$$\Delta\tau_j^k(t) = \lambda^k.Q/L_N \tag{8}$$

the pheromone change that ant No. k released at t instant along route L_N , and the weight coefficient lambda are represented by $\Delta\tau_j^k(t)$.

3.3. The ant colony optimization rw neural network

The ant colony optimization rw algorithm is a global optimization method. The weight coefficient and the concept of global regeneration were both used. There are several issues with the back propagation neural network algorithm, and therefore we utilize it as a training method for neural networks. For example, if there are m parameters in the neural network and the components of ants in the ant colony; this means that the neural network has all conceivable weights and thresholds values, and each of these parameters has m parameters. Set the neural network parameter $q_i(1 \leq i \leq m)$ to a m random nonzero value and create a set first I_{qi}. Weights and threshold values are selected by each individual, assuming that the ant in the group is free to determine transfer probability and concentration are factors that affect the parameters. Finally, they make it to their food supply and replenish the concentration of pheromones and parameters in order to get back on track. In the following table, the formulae have been changed:

$$\Delta\tau^k(I_{qi}) = \lambda^k.Q/e^k \tag{9}$$

$$e^{kj} = (O_s - O_I)2/2 \tag{10}$$

$\Delta\tau_j^k(I_{qI})$ is the change in pheromone concentration that ant k chooses No. j element in set I_{qI}; Q is constant, which is used to the adjustment speed of pheromone; e^k is the O/P error of the neural network, O_s is the actual O/P of neural network, O_I) is the expectation O/P of neural network; λ is weight index. The transfer probability will be used to renew the the global optimization path and individual optimization path. Once and for all, bring back the days of iteration. Figure 2 depicts the algorithm's flow chart.

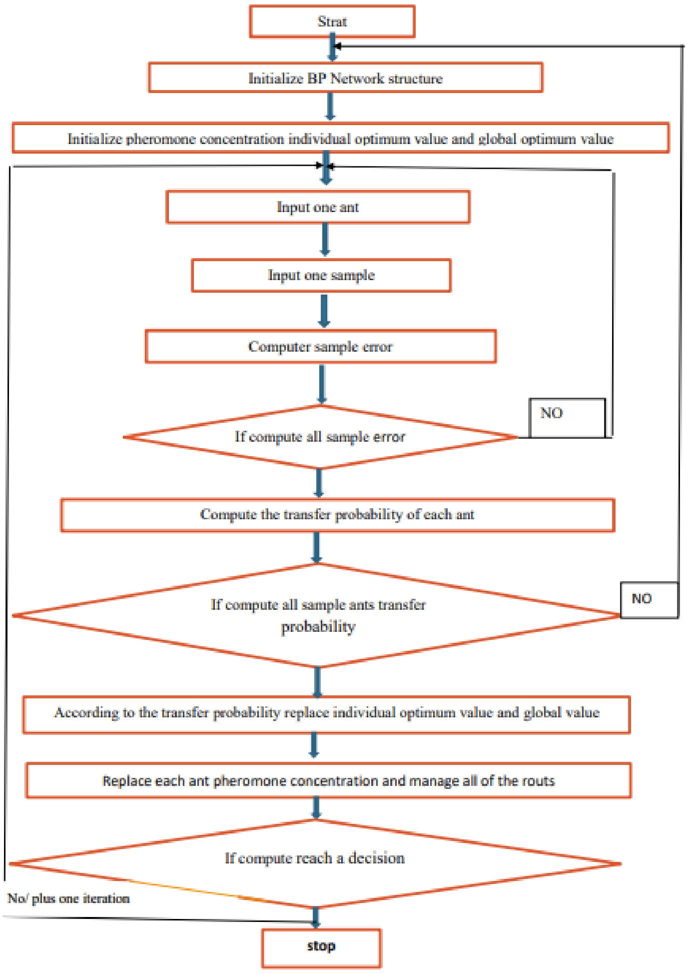

Figure 2. The new ant colony optimization-BP flow diagram

4. EXPERIMENT IN SIMULATION

4.1. Setup of the simulation parameters

Because of the variable nature of the hidden layer in BP neural networks, the value of the amount m of nodes can only be determined by trial and error. The experience formula may be used to determine the starting value 0 of the hidden layer nodes. To fine-tune the output error of neural networks, the hidden layer nodes may be added or removed during training. Many investigations have shown that the three-layer $M =$

$30, \lambda = 0.5$, and $\rho = 0.2$ have a large number of buried layer nodes, indicating that the claimed accuracy is 0.005. The starting state has a significant impact on the algorithm in this kind of search. In other words, we need to choose a good starting point. There is no practical purpose for this information in the DTC system since it is utilized in the ant colony optimization algorithm. MATLAB/Simulink is required to set up implement the sample cycle system and the DTC system simulation platform : It is important to note that the parameters of an AC motor are as follows: power rating: P_N=1.5 kw, voltage rating: V_N=380 v, frequency rating: f_N=50 Hz, inductance rating: L_s=0.0025 H, inductance rating: R_s=4.25 Ω and rotor resistance: R_r=3.24 Ω J=0.085 kg.m^2.

4.2. Algorithm to algorithm comparison

In training, a total of 2,000 sets of data are used as training samples. The maximum number of training sessions is set at 2,000, while the lowest possible level of error is set at 0.005. Table 1 shows the results of comparing the the ant colony optimization-BP with the single back propagation neural network employed in this work.

Table 1. Errors in the algorithum training

Name of algorithm	Predicted durations of training	The amount of time spent iterating	Error
BP	2005	1998	0.3980
Ant colony optimization -BP	2005	530	0.0040
Ant colony optimization rw-BP	2005	120	0.0039

When look at Tabel 1, have been notice that the single back propagation neural network training is taking a long time to attain its expected accuracy. Accuracy is achieved, however the ant colony optimization-BP takes longer to run than the ant colony optimization rw-BP used in this research. As a result, the redesigned ant colony optimization NN not only has a faster convergence speed, but also shorter iteration periods, and its accuracy is clearly improved.

A spike and burr can be seen in the single back propagation neural network 's training track curve by comparing Figure 3 with Figure 4, Figure 5, and Figure 6. Although the ant colony optimization-surge BP's and burr have been decreased, there is a time delay in the speed track curve and the track impact is negative. A superior track effect is achieved by using ant colony optimization rw-training BP's track curve, which does not have any burr. The foregoing findings show that ant colony optimization rw-capacity BP's to achieve the optimization effect is superior than that of both ant colony optimization-BP and single back propagation neural network , as seen from the data shown.

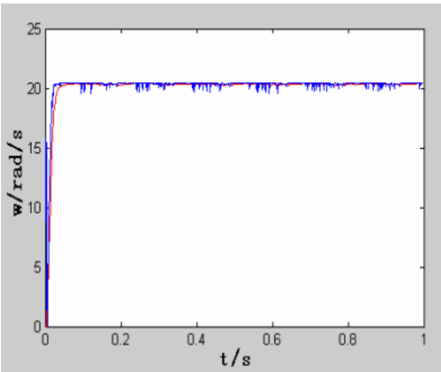

Figure 3. A single back propagation neural network's off-line training curve

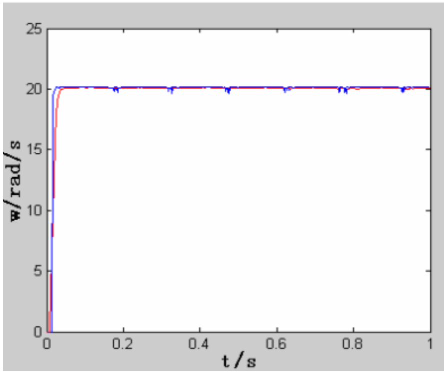

Figure 4. Ant colony optimization-off-line back propagation neural network's training curve

4.3. Internet-based training

In the DTC system of sensor less, we can retrieve the online track curve of flux linkage and speed by running the modified ant colony optimization rw-back propagation neural network, the single back propagation neural network into the simulation platform to run online and the ant colony optimization -back propagation neural network. According to Figures 6 to 11, they are From the graphs, we can observe that the single back propagation neural network's online identification curve has burr and spike. Online identification of the ant colony optimization-back propagation neural network has no surge or burr, but the identification effect is not optimal and there seems to be a time delay clearly. This paper's updated ant colony optimization rw-back propagation neural network speed identification is more accurate at tracking the real speed of a vehicle than the original. In $\alpha - \beta$ coordinate, the flux linkage track also has a smoother surface. This means that the ant colony optimization rw-back propagation neural network utilized in this research has excellent capability, and the speed identification built using the ant colony optimization rw-back propagation neural network has accomplished the DTC system of speed sensorless. The system's dynamic and static capabilities have been significantly improved.in the Figure 7 and Figure 8 the result proved the accuracy of speed by using -back propagation neural whereas Figure 9 and Figure 10 depicts back propagation neural network in the linkage flux.

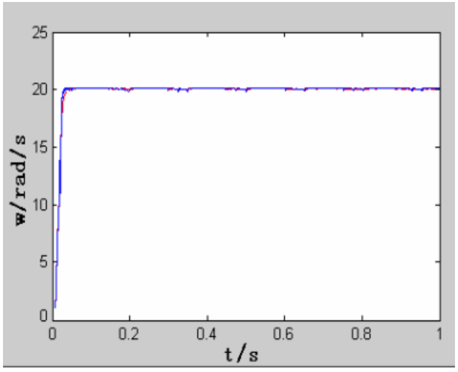

Figure 5. Updated ant colony optimization rw-off-line back propagation neural network 's training path curve

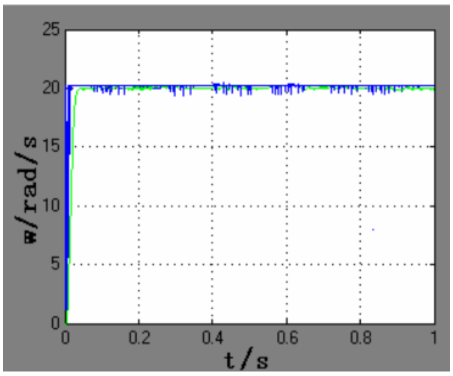

Figure 6. Cradle of one back propagation neural network 's online velocity identification

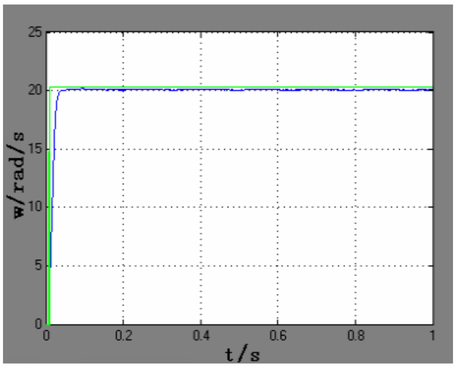

Figure 7. Identification curve for the online speed of the ant colony optimizatio -back propagation neuralnetwork

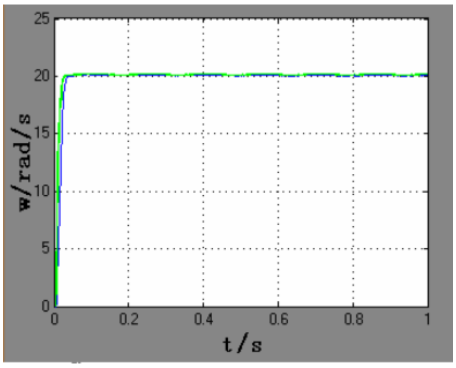

Figure 8. The ant colony optimization rw-back propagation neural network speed identification curve hasbeen updated

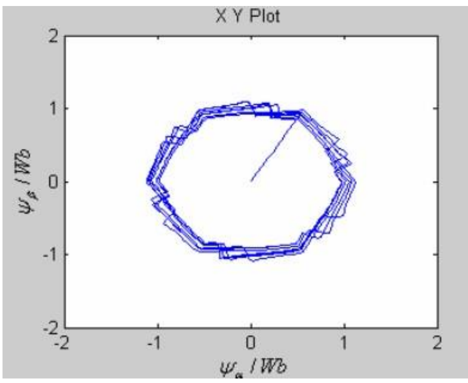

Figure 9. The single back propagation neural network's flux linkage curve

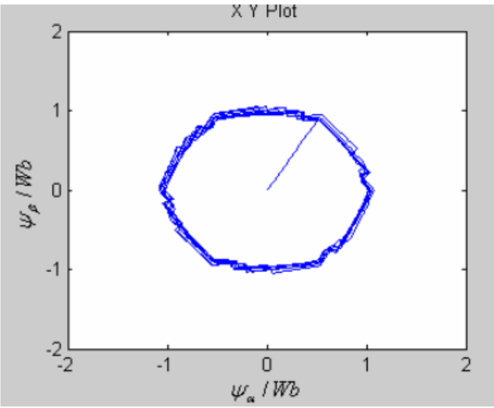

Figure 10. Linkage flux curve for ant colony optimization and back propagation neural network

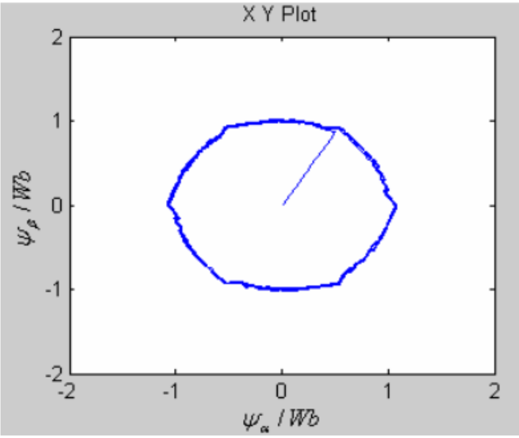

Figure 11. Linkage curve of the modified ant colony optimization rw-back propagation neural network flux

5. CONCLUSION

In this work, have been present the ant colony optimization rw-back propagation neural network model. Using the ant colony optimization rw-back propagation neural network in DTC highlights the fine capabilities of this method in recognizing non-linear functions, while also demonstrating the ant colony optimization 's capacity to speed up the back propagation neural network's avoid the local minimum point and convergence speed. The simulation results revealed that the speed sensor replaced with the ant colony optimization rw-optimized back propagation neural network -speed identification. Consequently, a useful project for the implementation of DTC speed sensor less has been created.

REFERENCES

[1] O.-D. Ramírez-Cárdenas and F. Trujillo-Romero, "Sensorless speed tracking of a brushless DC motor using a neural network," *Mathematical and Computational Applications*, vol. 25, no. 3, p. 57, Sep. 2020, doi: 10.3390/mca25030057.

[2] V. M. V. Rao and A. A. Kumar, "Artificial neural network and adaptive neuro fuzzy control of direct torque control of induction motor for speed and torque ripple control," in *2018 2nd International Conference on Trends in Electronics and Informatics (ICOEI)*, May 2018, vol. 13, pp. 1416–1422, doi: 10.1109/ICOEI.2018.8553871.

[3] S. M. Suryanarayana, B. Robertson, and S. Grillner, "The neural bases of vertebrate motor behaviour through the lens of evolution," *Philosophical Transactions of the Royal Society B: Biological Sciences*, vol. 377, no. 1844, p. 20200521, Feb. 2022, doi: 10.1098/rstb.2020.0521.

[4] O. Rodriguez-Abreo, J. Rodriguez-Resendiz, C. Fuentes-Silva, R. Hernandez-Alvarado, and M. D. C. P. T. Falcon, "Self-tuning neural network pid with dynamic response control," *IEEE Access*, vol. 9, pp. 65206–65215, 2021, doi: 10.1109/ACCESS.2021.3075452.

[5] A. J. Ali, A. M. T. Ibraheem, and O. T. Mahmood, "Design of a smart control and protection system for three-phase generator using Arduino," *IOP Conference Series: Materials Science and Engineering*, vol. 745, no. 1, p. 012027, Feb. 2020, doi: 10.1088/1757-899X/745/1/012027.

[6] B. A. Hamad, A. M. T. Ibraheem, and A. G. Abdullah, "Design and practical implementation of dual-axis solar tracking system with smart monitoring system," *Przeglad Elektrotechniczny*, vol. 96, no. 10, pp. 151–155, Oct. 2020, doi: 10.15199/48.2020.10.28.

[7] B. Sahoo, S. K. Routray, P. K. Rout, and M. M. Alhaider, "Advanced adaptive filter-based control strategy for active switch inverter operation," in *Lecture Notes in Electrical Engineering*, vol. 814, 2022, pp. 183–195.
[8] V. F. Pires, A. Cordeiro, D. Foito, and A. J. Pires, "Fault-tolerant multilevel converter to feed a switched reluctance machine," *Machines*, vol. 10, no. 1, p. 35, Jan. 2022, doi: 10.3390/machines10010035.
[9] K. B. Tawfiq, M. N. Ibrahim, and P. Sergeant, "An enhanced fault-tolerant control of a five-phase synchronous reluctance motor fed from a three-to-five-phase matrix converter," *IEEE Journal of Emerging and Selected Topics in Power Electronics*, pp. 1–1, 2022, doi: 10.1109/JESTPE.2022.3148188.
[10] Z. Ping, M. Zhou, C. Liu, Y. Huang, M. Yu, and J.-G. Lu, "An improved neural network tracking control strategy for linear motor-driven inverted pendulum on a cart and experimental study," *Neural Computing and Applications*, vol. 34, no. 7, pp. 5161–5168, Apr. 2022, doi: 10.1007/s00521-021-05986-9.
[11] M. Chaput *et al*., "Visual cognition associated with knee proprioception, time to stability, and sensory integration neural activity after ACL reconstruction," *Journal of Orthopaedic Research*, vol. 40, no. 1, pp. 95–104, Jan. 2022, doi: 10.1002/jor.25014.
[12] Y. G. Rashid and A. M. A. Hussain, "Implementing optimization of PID controller for DC motor speed control," *Indonesian Journal of Electrical Engineering and Computer Science*, vol. 23, no. 2, p. 657, Aug. 2021, doi: 10.11591/ijeecs.v23.i2.pp657-664.
[13] A. M. T. I. Alnaib, O. T. M. Altaee, and N. A. A. B. Al-Jawady, "PLC controlled multiple stepper motors using various excitation methods," *International Iraqi Conference on Engineering Technology and its Applications, IICETA 2018*, pp. 54–59, 2018, doi: 10.1109/IICETA.2018.8458097.
[14] Z. S. Mahmood, I. B. Kadhim, and A. N. Nasret, "Design of rotary inverted pendulum swinging-up and stabilizing," *Periodicals of Engineering and Natural Sciences (PEN)*, vol. 9, no. 4, p. 913, Nov. 2021, doi: 10.21533/pen.v9i4.2453.
[15] Z. S. Mahmood, A. N. Nasret, and O. T. Mahmood, "Separately excited DC motor speed using ANN neural network," in *AIP Conference Proceedings*, 2021, vol. 2404, p. 080012, doi: 10.1063/5.0068893.
[16] P. Sutyasadi and M. Parnichkun, "Developing low-cost two wheels balancing scooter using proportional derivative controller," *International Journal of Electrical and Computer Engineering (IJECE)*, vol. 12, no. 3, p. 2454, Jun. 2022, doi: 10.11591/ijece.v12i3.pp2454-2464.
[17] A. Kirad, S. Grouni, and Y. Soufi, "Improved sensorless backstepping controller using extended Kalman filter of a permanent magnet synchronous machine," *Bulletin of Electrical Engineering and Informatics*, vol. 11, no. 2, pp. 658–671, Apr. 2022, doi: 10.11591/eei.v11i2.3560.
[18] J. A. Barrios, F. Sanchez, F. Gonzalez-Longatt, and G. Claudio, "System identification applied to a single area electric power system under frequency response," *Indonesian Journal of Electrical Engineering and Computer Science*, vol. 22, no. 3, p. 1236, Jun. 2021, doi: 10.11591/ijeecs.v22.i3.pp1236-1244.
[19] S. Surya, S. P., and S. S. Williamson, "A comprehensive study on DC–DC and DC–AC converters in electric and hybrid electric vehicles," in *EAI/Springer Innovations in Communication and Computing*, 2022, pp. 59–81.
[20] E. Robles, M. Fernandez, J. Andreu, E. Ibarra, J. Zaragoza, and U. Ugalde, "Common-mode voltage mitigation in multiphase electric motor drive systems," *Renewable and Sustainable Energy Reviews*, vol. 157, p. 111971, Apr. 2022, doi: 10.1016/j.rser.2021.111971.
[21] B. Sirisha and M. A. Nazeemuddin, "A novel five-level voltage source inverter interconnected to grid with srf controller for voltage synchronization," *Bulletin of Electrical Engineering and Informatics*, vol. 11, no. 1, pp. 50–58, Feb. 2022, doi: 10.11591/eei.v11i1.3274.
[22] A. U. Rehman, B. A. Basit, H. H. Choi, and J.-W. Jung, "Computationally efficient deadbeat direct torque control considering speed dynamics for a surface-mounted PMSM drive," *IEEE/ASME Transactions on Mechatronics*, pp. 1–12, 2022, doi: 10.1109/TMECH.2021.3140077.
[23] A. Hota and V. Agarwal, "A new three-phase inverter topology for reducing the dv/dt and peak-to-peak Value of Common Mode Voltage," *IEEE Transactions on Industrial Electronics*, vol. 69, no. 12, pp. 11979–11986, Dec. 2022, doi: 10.1109/TIE.2022.3140517.
[24] N. M. Abbas, D. N. Saleh, and A. M. Shakor, "Three phase induction motor torque tracking algorithm based on the rotor time constant identification," *Indonesian Journal of Electrical Engineering and Computer Science*, vol. 25, no. 3, pp. 1320–1327, Mar. 2022, doi: 10.11591/ijeecs.v25.i3.pp1320-1327.
[25] S. Alepuz *et al.*, "A survey on capacitor voltage control in neutral-point-clamped multilevel converters," *Electronics (Switzerland)*, vol. 11, no. 4, p. 527, Feb. 2022, doi: 10.3390/electronics11040527.
[26] K. Sayed, A. Almutairi, N. Albagami, O. Alrumayh, A. G. Abo-Khalil, and H. Saleeb, "A review of DC-AC converters for electric vehicle applications," *Energies*, vol. 15, no. 3, p. 1241, Feb. 2022, doi: 10.3390/en15031241.
[27] V. Jain, J. P. Keshri, H. Tiwari, and Pankaj, "Five-level single-phase converter using SiC with reduced switched voltage stress," in *Lecture Notes in Electrical Engineering*, vol. 766, 2022, pp. 327–337.

BIOGRAPHIES OF AUTHORS

Arshad B. Salih received a B.S. in Electronics and Control Engineering from Kirkuk technical college, Iraq, in 2007, and M.S. degree in Electronic and Communication Engineering from Istan- bul University, Turkey, in 2011. He is an lecturer in northern technical university Kirkuk technical institute from 2017 to the present. He can be contacted at email: arshadsalih@ntu.edu.iq.

Zuhair Shakor Mahmood received a B.S. in Electronics and Control Engineering from Kirkuk technical college, Iraq, in 2005, and M.S. degree in Electrical and Electronic Engineering from Eskishir Osmangazi University, Turkey; in 2012, He is a lecturer in northern technical university Kirkuk institute from 2017 to the present. He can be contacted at email: zuherkazanci@ntu.edu.iq.

Ardm Haseeb Mohammed Ali received a B.S. in Electronics and Control Engineering from Kirkuk technical college, Iraq, in 2003, and M.S. degree in Electronic and Communication Engineer- ing from Cankaya University, Turkey, in 2012.and the Ph.D degree from cankaya university in 2017 He is an lecturer in imam al ajafaar sadiq university from 2017 to the present. He can be contacted at email: ardmmohammed@sadiq.edu.iq.

Ali Najdet Nasret received B.S. in Electrical Engineering from Al-mustansriya Uni- veristy, Iraq, in 2010, and M.S. degree in Electronic and Communication Engineering from Cankaya University, Turkey, in 2014. He is an lecturer in northern technical university Kirkuk technical insti- tute from 2017 to the present. He can be contacted at email: alinajdet@ntu.edu.iq.